Simultaneous surface topography and spin-injection probability

D. W. Bullock,[a] V. P. LaBella, Z. Ding, and P. M. Thibado
Department of Physics, The University of Arkansas, Fayetteville, Arkansas 72701

(Received 9 August 2002; accepted 28 October 2002; published 23 December 2002)

A spin-polarized electron current is injected into a *p*-type GaAs(110) surface at 100 K using a polycrystalline ferromagnetic Ni scanning tunneling microscope tip. The injected electrons recombine to the valence band and emit circularly polarized light, and the degree of the light polarization is related to the degree of the electron polarization at the instant of recombination. Details of how to simultaneously measure the surface topography and obtain a pixel-by-pixel map of the spin-injection probability are discussed. The degree of light polarization is found to change when the electrons are injected into a clean, flat terrace versus over a step. However, the terrace-to-step polarization differences are systematically reduced as the energy of the electron is reduced. [DOI: 10.1116/1.1532022]

I. INTRODUCTION

The prospects of developing next generation semiconductor devices that utilize the spin of the electron, i.e., ''spintronic'' devices, has led to a flurry of research activity.[1–5] For electronics to utilize the spin, three features of the device structure must be met. First, a spin-polarized current is needed. Second, the electron spin must be coherently injected into a semiconductor. Third, the polarization of the electrons must be maintained while traveling through the device. The most difficult challenge involves the efficient injection of spin-polarized electrons from a ferromagnetic material into a nonmagnetic semiconductor. Both ferromagnetic semiconductors and ferromagnetic metals offer great promise as sources for the spin-polarized currents. Ferromagnetic semiconductors have shown injection efficiencies as high as 90%, however, these materials have low Curie temperatures ($\sim$40 K).[6–8] Ferromagnetic metal current sources remain magnetic at high temperatures, but yield low spin-injection probabilities.[9,10] The low probability is thought to be due to chemical intermixing that occurs when the metal comes in contact with the semiconductor.

A natural instrument that lends itself well to studying interface issues is the scanning tunneling microscope (STM). Alvarado *et al.* used point-mode STM to study the spin-injection properties of a ferromagnetic Ni tip into the GaAs(110) surface by measuring the time-integrated polarization of the recombination luminescence.[11–13] We have recently extended this technique to take advantage of the high-spatial resolution capability of the STM, to show how atomically abrupt steps can significantly reduce the spin-injection probability.[14]

In this article we take advantage of the extra space to explain in detail how one can carry out simultaneous topography and pixel-by-pixel maps of the electron spin-injection probability. Furthermore, we show that the difference in the spin-injection probability between a flat terrace and a step is reduced as the energy of the tunneling electron is reduced.

[a]Electronic mail: dbulloc@uark.edu

II. EXPERIMENT

The overall strategy of this experiment is to use a spin-polarized electron source to locally inject electrons into a *p*-type GaAs(110) surface. By measuring the degree of circular polarization of the recombination luminescence, information about the local spin-injection properties can be obtained.

A polarized electron current is generated from ferromagnetic polycrystalline Ni wire. The wire was electrochemically etched under high magnification (500 $\times$) using a 10% HCl solution then loaded into an ultrahigh vacuum (UHV) chamber [$(4-8)\times10^{-11}$ Torr] that contains a commercially available (Omicron) variable-temperature scanning tunneling microscope (VTSTM). The tips were then cleaned *in situ* using electron-beam heating and placed on the STM imaging stage. For control purposes, nonmagnetic single-crystal $\langle 111\rangle$-oriented W tips were used and etched with NaOH, but otherwise prepared in the same manner as the Ni tips. The GaAs(110) surface was prepared by cleaving *p*-type GaAs(001) wafers (Zn doped, $p=1.25\times10^{19}$ cm^{-3}) *in situ* which produces a clean, nearly atomically flat cross-sectional (110) surface. The sample was then placed on the STM stage where it was cooled via a cold finger immersed in LN_2. The sample temperature is estimated to be $\sim$100 K.

Electrons are injected into the empty conduction band states of GaAs. They eventually recombine across the 1.49 eV fundamental band gap emitting light which is collected using a f/1.0, biconvex lens, as illustrated in the upper half of Fig. 1. The lens is mounted *in situ* and positioned 12.7 mm from the STM tip (the focal length of the lens). The position of the lens was optimized using a three-axis translational, and two-axis rotational external micrometer controlled wobble-stick. After passing through the lens, the light is transmitted through an UHV viewport to polarization sensitive optics. The optics contain a $\lambda/4$ retarder fastened in a two position mount. The first position (A) converts right-circularly polarized (RCP) light to a horizontal linear component and the left-circularly polarized (LCP) light to a vertical linear component, while the second position (B) does the opposite, as displayed in the lower half of Fig. 1. The

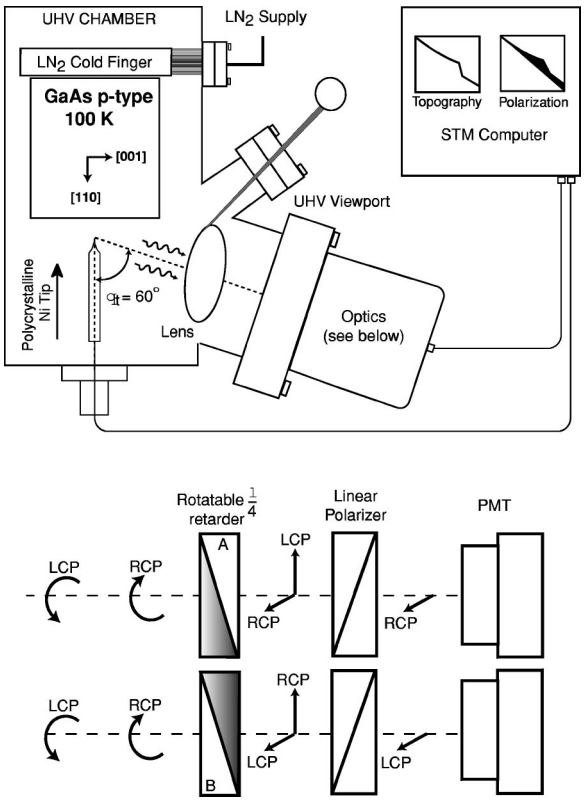

FIG. 1. (above) Schematic diagram of the experimental setup used to inject a spin-polarized current into the GaAs(110) surface and detect the circularly polarized recombination luminescence. (below) Schematic diagram of the optical system used to convert right and left circularly polarized light into linearly polarized light, so that the intensity of both the right and left can be independently determined.

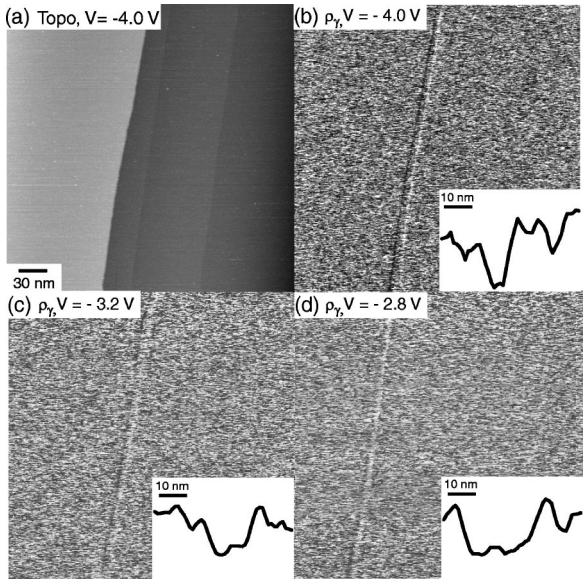

FIG. 2. (a) A 300×300 nm^2 empty state STM image using a polycrystalline Ni tip with a sample bias of -4.0 V and tunneling current of 6 nA. The sample temperature is assumed to be at 100 K, and gray levels represent a height change of about 2.9 nm. (b)–(d) 400 pixel by 400 pixel images of the degree of circularly polarized luminescence, $\rho_\gamma=(I_{\mathrm{LCP}}-I_{\mathrm{RCP}})/(I_{\mathrm{LCP}}+I_{\mathrm{RCP}})$, taken simultaneously with the topography data at a sample bias of -4.0 V, -3.2 V, and -2.8 V, respectively. The gray levels represent a change in optical polarization of 11%. Inset line profiles were extracted across the trench from the degree of polarization images and shown magnified.

linear polarizer passes only the horizontal linear component to a high-sensitivity cooled photomultiplier tube (PMT) configured to convert ~4000 photons/s to 1 nA of current. In this way, by manually switching between position (A) and (B) the intensities of the RCP and LCP light are measured.

The current from the PMT is measured using the STM computer. The STM computer is configured to simultaneously read the PMT signal, as it measures the topography. This provides a detailed topographical map of the surface and a corresponding map of the intensities of the polarized light at the local position of the STM tip. Typically, multiple sets of images in one area are acquired with the polarizer alternately in position (A) and (B) to obtain an average of both the pixel-by-pixel RCP and LCP light intensities, respectively.

III. RESULTS

A typical empty-state STM image (300×300 nm^2) taken with a sample bias of -4.0 V and tunneling current of 6 nA is shown in Fig. 2(a). The tunneling current is set this high to increase the optical signal, and these tunneling conditions did not effect the reproducibity of data sets taken sequentially. This grayscale image shows multiple terraces separated by steps of varying height running vertically through the middle of the image. Starting from the highest terrace on the left side of the image, the first step has a height change of 2.9 nm and is followed by two smaller monolayer high steps. Multiple two-dimensional grayscale images of the degree of circular luminescence polarization, as a function of tunneling bias, are shown in Figs. 2(b)–2(d). To calculate the pixel-by-pixel luminescence polarization, the intensity images for the LCP (I_{LCP}) and RCP (I_{RCP}) light data were first corrected for any drift that may have occurred between scans. Then, a pixel-by-pixel subtraction of the RCP image from the LCP image was performed. In a similar manner, the two images were added together, and the polarization was calculated by a pixel-by-pixel division, resulting in a two-dimensional, 400 pixel$\times$400 pixel map of the polarization denoted by $\rho_\gamma=(I_{\mathrm{LCP}}-I_{\mathrm{RCP}})/(I_{\mathrm{LCP}}+I_{\mathrm{RCP}})$. The resulting images have a black-to-white colorscale that represents an optical polarization change, $\Delta\rho_\gamma$, of 11% in Figs. 2(b)–2(d). These grayscale images show fluctuations on the terraces, however, a significant decrease in polarization for Fig. 2(b) is observed at the largest step edge, while no noticeable effect occurs for the monolayer high steps. As the tunneling voltage is decreased the change in polarization at the step edge becomes less evident as shown in Figs. 2(c) and 2(d).

IV. DISCUSSION

STM spin injection followed by optical polarization measurements have been done before using time-integration methods.[11–13] The authors have developed a technique for simultaneously acquiring topographic and light intensity data

in real time, however, due to previous space limitations the details of how to reproduce this experiment were not discussed.[14] In this paragraph, we provide those details. The first thing to consider is how many photons can one expect to collect. Typical STM tunneling currents of ~1 nA result in $\sim 10^{10}$ e^-/s being injected into the conduction band. Assuming (for now) that each electron recombines to the valence band by emitting a photon, $\sim 10^{10}$ photons/s can be expected. The first lens used in the optical setup described here captures ~5% of the total solid angle. Critical to obtaining this large value was a custom designed *in situ* five-axis micrometer controlled lens mount. Even still, the photons are generated a few microns inside the GaAs sample, and some are lost due to reflection at the GaAs–vacuum interface. In addition, refraction causes the photons that are transmitted to be bent away from the normal, further reducing the optical collection efficiency. All totalled, the collected photon intensity is decreased to $\sim 10^8$ photons/s, however, this is still neglecting the optical diffraction that will occur due to the presence of the metal tip. Under normal scanning conditions, the STM tip only collects data for a few hundred microseconds at each pixel location, which can lead to only a few ten-thousand photons/pixel. A preliminary test at room temperature did not reveal this level of photon intensity. The reason for this is well-known, and is due to microscopic defects forming a continuum of states due to thermal broadening at high temperatures.[15] One can obtain at least a factor of 10 increase in the optical signal by working at 100 K. In summary, we found this difficult experiment is doable, yet the analysis is complicated.

This experiment not only requires measuring the intensity of the emitted light, but also its polarization. Polarized light is emitted from GaAs because of the large spin-orbit splitting in the valence band.[11,16–18] Naturally, the degree of the circular polarization of the light, ρ_γ depends upon the degree of polarization of the electrons when they recombine, ρ_e. In this study, of primary interest is the change in polarization across the surface, which is given by

$$\Delta\rho_e = 2\Delta\rho_\gamma/\cos(\theta_i), \tag{1}$$

where θ_i is the polar angle between the direction that the electron spin is pointing and the propagation direction of the emitted light.[11,14,19] This angle is related to the detection angle through Snell's law,

$$\theta_i = \sin^{-1}\left(\frac{n_{\mathrm{vac}}}{n_{\mathrm{GaAs}}\sin(\theta_t)}\right), \tag{2}$$

where n_{vac} and n_{GaAs} are the indexes of refraction of the vacuum and GaAs substrate, respectively, and θ_t is the angle between the detection optics and the sample normal, as shown in Fig. 1.[11,18,20] Substituting $n_{\mathrm{vac}}=1.0$, $n_{\mathrm{GaAs}}=3.3$, and $\theta_t=60°$ into Eq. (2), θ_i is found to be 15.4°. Using this value in Eq. (1) results in

$$\Delta\rho_e = 2.1\Delta\rho_\gamma, \tag{3}$$

which relates the electron polarization at the time of recombination to the measured optical polarization. Thus the images of the optical polarization shown in Figs. 2(b)–2(d) are also images of the electron spin polarization, where the gray scale represents a change in electron spin polarization of $\Delta\rho_e = 23\%$. Effectively, we now have a two-dimensional map of the electron spin-injection probability, which visually displays the atomic-scale features that affect the coherent transfer of spins from a ferromagnetic metal through a vacuum and into a semiconductor.

Based on the new information that the gray scale changes in the images shown in Figs. 2(b)–2(d) represent changes in the electron spin-injection probability, the meaning of the data shown in Fig. 2(b) is first discussed. The position of the large topographical step shown in Fig. 2(a) directly corresponds to a decrease in the polarization of the injected electrons. It is also interesting that the monolayer high steps that appear in Fig. 1(a) do not have a measurable effect on the polarization data. This indicates that feature size (not just the type of feature) has an effect on spin-injection probability. An enhancement in the spin scattering at large step edges is most likely due to the larger number of dangling bonds on the side surface of the step. If the dangling bonds are half occupied, then the electron's spin on the surface can cause a spin-spin scattering event with the injected electron.

In this experiment, the spatial effects of lowering the sample bias on the spin-injection probability are shown in Figs. 2(b)–2(d). Lowering the sample bias (which lowers the energy of the tunneling electron) reduced the effect the step edge has on disrupting the spin-injection process. As the bias is lowered (in constant current mode), the tunneling distance is reduced. As the tip gets closer to the sample the effective tunneling area of the tip is increased. This results in a larger angular spread in the tunneling electrons moving from the tip to the sample. It is known that electrons moving along different crystallographic directions in Ni have different polarizations.[21] Consequently, it is likely that side tunneling from the tip enhances the effective polarization of the tunneling current, thereby accounting for the decrease in the change in polarization between the step and terrace.

V. CONCLUSION

By combining spin-polarized, low-temperature STM with polarization sensitive optics, it was demonstrated that one can measure both the atomic-scale topography and a corresponding pixel-by-pixel map of the spin-injection probability. Details of the experimental setup are given, as well as the theoretical considerations that must go into the analysis of the results. We report that steps of significant height can disrupt the electron spin-injection process on the atomic scale. This information may play a critical role in understanding how to one day make commercial spintronic devices.

ACKNOWLEDGMENTS

This work is supported by the National Science Foundation under Grant No. FRG DMR-0102755 and C-Spin MRSEC DMR-0080054, as well as by the Office of Naval Research under Grant No. N00014-97-1-1058.

[1]S. Datta and B. Das, Appl. Phys. Lett. **56**, 665 (1990).
[2]G. A. Prinz, Phys. Today **48**, 58 (1995).
[3]D. D. Awschalom and J. M. Kikkawa, Phys. Today **52**, 33 (1999).
[4]G. A. Prinz, Science **250**, 1092 (1990).
[5]H. Ohno, Science **281**, 951 (1998).
[6]R. Fiederling, M. Keim, G. Reuscher, W. Ossau, G. Schmidt, A. Waag, and L. W. Molenkamp, Nature (London) **402**, 787 (1999).
[7]Y. Ohno, D. K. Young, B. Beschoten, F. Matsukura, H. Ohno, and D. D. Awschalom, Nature (London) **402**, 790 (1999).
[8]B. T. Jonker, Y. D. Park, B. R. Bennett, H. D. Cheong, G. Kioseoglou, and A. Petrou, Phys. Rev. B **62**, 8180 (2000).
[9]P. R. Hammar, B. R. Bennett, M. J. Yang, and M. Johnson, Phys. Rev. Lett. **83**, 203 (1999).
[10]A. T. Hanbicki, B. T. Jonker, G. Itskos, G. Kioseoglou, and A. Petrou, Appl. Phys. Lett. **80**, 1240 (2002).
[11]S. F. Alvarado and P. Renaud, Phys. Rev. Lett. **68**, 1387 (1992).
[12]S. F. Alvarado, Phys. Rev. Lett. **75**, 513 (1995).
[13]S. F. Alvarado, in *New Trends in Magnetism Magnetic Materials and Their Applications*, edited by J. Moran-Lopez and J. Sanchez (Plenum, New York, 1994), pp. 175–182.
[14]V. P. LaBella, D. W. Bullock, Z. Ding, C. Emery, A. Venkatesan, W. F. Oliver, G. J. Salamo, P. M. Thibado, and M. Mortazavi, Science **292**, 1518 (2001).
[15]J. I. Pankove, *Optical Processes in Semiconductors* (Prentice-Hall, Englewood Cliffs, NJ, 1971).
[16]R. C. Miller, D. A. Kleinman, W. A. Nordland, Jr., and R. A. Logan, Phys. Rev. B **23**, 4399 (1981).
[17]K. Zerrouati, F. Fabre, G. Bacquet, J. Bandet, J. Frandon, G. Lampel, and D. Paget, Phys. Rev. B **37**, 1334 (1988).
[18]D. T. Pierce and F. Meier, Phys. Rev. B **13**, 5484 (1976).
[19]D. W. Bullock, V. P. LaBella, Z. Ding, and P. M. Thibado, J. Supercond. **15**, 37 (2002).
[20]W. F. Egelhoff, M. D. Stiles, D. P. Pappas, D. T. Pierce, J. M. Byers, M. B. Johnson, B. T. Jonker, S. F. Alvarado, J. F. Gregg, J. A. C. Bland, and R. A. Buhrman, Science **296**, 1195 (2002).
[21]E. Kisker, W. Gudat, E. Kuhlmann, R. Clauberg, and M. Campagna, Phys. Rev. Lett. **45**, 2053 (1980).